

Optimizing the thermoelectric properties of PEDOT:PSS films by combining organic co-solvents with inorganic base

Zhengyou Zhu¹ · Congcong Liu¹ · Qinglin Jiang¹ · Hui Shi¹ · Fengxing Jiang¹ · Jingkun Xu¹ · Jinhua Xiong¹ · Endou Liu¹

Received: 22 April 2015 / Accepted: 20 July 2015 / Published online: 25 July 2015
© Springer Science+Business Media New York 2015

Abstract A simple optimizing approach that effectively improves the thermoelectric performance of poly(3,4-ethylenedioxythiophene):poly(styrenesulfonate) (PEDOT:PSS) films is presented in this paper. The optimizing process is performed by over-dropping a mixture of DMSO/NaOH ethanol solution onto the PEDOT:PSS films, achieving the facile combination of co-solvents effect and dedoping effect. Largely varied electrical conductivity from 837.2 to 0.04 S cm⁻¹ and the Seebeck coefficient from 12.6 to 54.8 μV K⁻¹ are observed by changing the ratios between DMSO and NaOH ethanol solution. Due to the precise control of the dedoping level of PEDOT chains, an optimized power factor of 33.04 μW m⁻¹ K⁻² is obtained at the ratio of 10:12 in volume, which is four orders of magnitude higher than that of the pristine film and more than twice the value of DMSO-treated one, simultaneously with the corresponding electrical conductivity and Seebeck coefficient being 598.2 S cm⁻¹ and 23.5 μV K⁻¹, respectively. Based on the measured thermal conductivity of 0.173 W m⁻¹ K⁻¹, the maximum *ZT* value is calculated to be 0.057 at room temperature.

1 Introduction

In the context that the global energy crisis and alarming environmental problems arise, thermoelectric (TE) materials have attracted significant interest in recent years due to their potential for generating power from waste heat [1–3]. A suitable TE material must be good at conducting electricity yet poor at conducting heat, the TE performance is characterized by a dimensionless figure of merit, expressed by $ZT = \sigma S^2 T / \kappa$, where σ , S , K and T represent the electrical conductivity, Seebeck coefficient, thermal conductivity, and absolute temperature, respectively [3–6]. Relative to conventional inorganic TE materials, conducting polymers possess unique features for application as TE materials because of their low density, low cost due to rich levels of resources, easy synthesis and facile processing into versatile forms [7].

Among the various organic TE materials investigated, poly(3,4-ethylenedioxythiophene):poly(styrenesulfonate) (PEDOT:PSS) as a promising conducting polymer which exhibits great potential as materials for TE applications has come to the fore front and has drawn intensive investigation recent years [8–13]. In 2008, our group firstly reported the thermoelectric performance of PEDOT:PSS, drawing a new research hotspot in the field of organic TE materials [11]. In spite of the intrinsic advantages of PEDOT:PSS, the conflicting combination among the electrical conductivity, Seebeck coefficient and the thermal conductivity imposes limitations on the optimization of *ZT*, hence its TE efficiency, however to date, is still much lower than that of inorganic semiconductor-based TE devices [5, 14, 15]. To obtain an excellent *ZT* value at room temperature, in addition to its intrinsic low thermal conductivity, a high power factor is also of key importance. Currently, a variety

Zhengyou Zhu and Congcong Liu have contributed equally to this work.

✉ Jingkun Xu
xujingkun@tsinghua.org.cn

¹ Jiangxi Key Laboratory of Organic Chemistry, Jiangxi Science and Technology Normal University, Nanchang 330013, China

of situations have been reported to improve the power factor thus the TE properties of PEDOT:PSS films, and they can be summarized as follows: 1st, remarkably enhanced electrical conductivity with a trivial change in the Seebeck coefficient by polar solvents treatment such as DMSO, EG etc. [16–19]. 2nd, a larger Seebeck coefficient with a relatively not notable electrical conductivity by a reduction method [20, 21]. 3rd, simultaneous enhancement in the electrical conductivity and Seebeck coefficient by post-treatment, mixing approach or blending with inorganic materials etc. [12, 14, 22–24]. 4th, optimization of power factor by controlling the redox level of PEDOT chains through a dedoping process [25–27].

Recently, several research groups have reported the TE enhancement of PEDOT:PSS films by controlling the dedoping level of PEDOT chains. For example, Tsai et al. [27] achieved the optimization of power factor of PEDOT:PSS films by NaOH addition into the polymer solution (5 vol% DMSO) for the first time. Lee et al. [28] optimized the oxidation level of PEDOT chains by sequential doping and dedoping process and obtained a high *ZT* value of 0.31. It is worth noting that Kim et al. [12] reported the highest *ZT* value of 0.42 for PEDOT:PSS films also by controlling the oxidation level via a dedoping method. All these recent significant breakthroughs in the TE performances of PEDOT came from the optimization method by controlling the oxidation level, which suggested that this technique was effective and promising. On the other hand, in a newly-published literature, Liu et al. [29] systematically investigated the effect of co-solvents consisting of DMSO and EG on the TE performances of PEDOT:PSS films. In fact, as previously reported, [29–33] co-solvents system has been confirmed to exhibit synergistic effect on physical properties of materials such as solubility, adsorption, micellar, liquefaction and electrical conductivity etc. due to the variation of dielectric constant, cohesive energy, and hydrogen bonding abilities of the system. Hence, it is believed that the introduction of co-solvents into the TE investigation of PEDOT:PSS is an interesting work and full of expectation.

Considering comprehensively, according to the ideas above, in this work we utilized a mixture of DMSO and EtOH which dissolved NaOH as a post-treatment reagent for the PEDOT:PSS films. Herein, organic DMSO/EtOH co-solvents and the inorganic base NaOH were acted as a dopant and dedopant respectively for the turning of electrical conductivity and Seebeck coefficient. Hence we have facily combined the co-solvents effect and dedoping effect. By precisely controlling the dedoping level of PEDOT chains, we have achieved an optimized power factor thus the improved TE properties. Furthermore, the origin and mechanism of the improvement were analyzed and discussed by various characterization methods.

2 Experimental

2.1 Materials

PEDOT:PSS aqueous solution (CLEVIOS PH1000) was purchased from H.C. Starck. The concentration of PEDOT:PSS was 1.3 % by weight, and the weight ratio of PSS to PEDOT was 2.5. Dimethyl sulfoxide (DMSO), ethanol and NaOH purchased from Beijing Chemical Plant (Beijing, China). These materials were used without further purification.

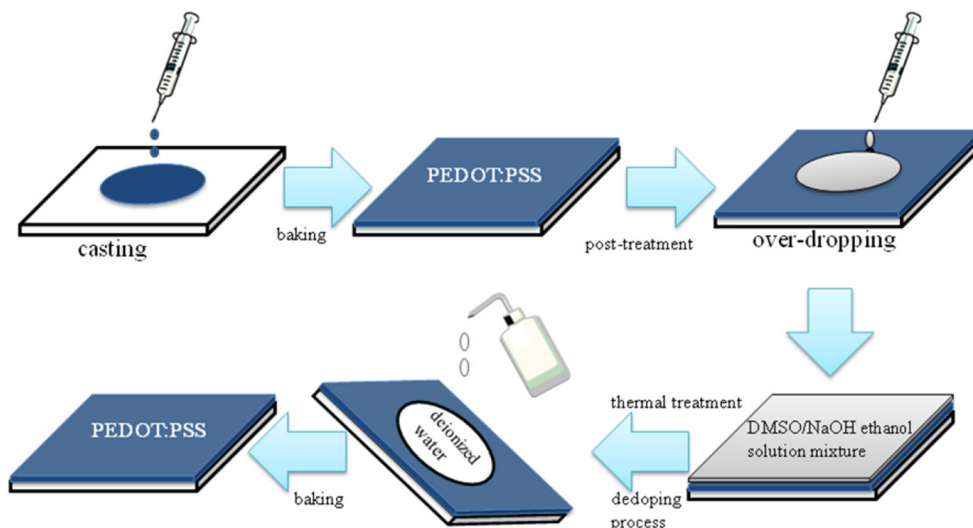
2.2 DMSO/NaOH ethanol solution mixture post-treatment

Pristine PEDOT:PSS films were prepared from the as-received PEDOT:PSS solutions by casting them on the pre-cleaned glass substrates ($2 \times 2 \text{ cm}^2$) then dried in vacuum oven at 60 °C for 12 h. DMSO/NaOH ethanol solution (0.125 M) mixtures were prepared by directly adding DMSO into NaOH ethanol solution. Post-treatment was performed by dropping the above mixtures with different volume ratios on the surfaces of the polymer films. After a thermal treatment under 80 °C for 10 h in ambient atmosphere, the film surfaces were rinsed thoroughly with deionized water and dried again for 3 h in a baking oven. The process of the post-treatment is shown in Fig. 1.

2.3 Measurements and characterizations

Electrical conductivity and Seebeck coefficient were measured with a homemade shielded four-point probe apparatus with a Keithley 2700 Multimeter (Cleveland, OH, USA) and a regulated DC power supply (MCH-303D-II, China) in conjunction with Labview (National Instruments, Austin, TX, USA). For electrical conductivity and Seebeck coefficient measurements, samples were cut into pieces of a rectangular shape (length, 20.0 mm; width, 4.0 mm) and suspended by using a thermal paste between two TE devices used for creating temperature difference. Electrical conductivity was measured by using a current-voltage (IV) sweeping measurement technique with four-point probes after four metal lines were patterned with a silver paint. For the Seebeck coefficient measurement, temperature gradients along the long edge of the sample were measured by two T-type thermocouples. The temperature and electrical potential differences are given by $\Delta T = T_{hot} - T_{cold}$, $\Delta V = V_{cold} - V_{hot}$, respectively. The Seebeck coefficient was calculated by $S = -(\Delta V / \Delta T)$. Temperature difference ΔT of about 5 K was used here in measurements. For other characterizations, the surface morphology was captured in tapping mode by Atomic

Fig. 1 Schematic diagram of the post-treatment process of PEDOT:PSS films



Force Microscopy (AFM, Veeco Multimode) and the surface compositions changes of the samples were analyzed using X-ray photoelectron spectroscopy (XPS, Thermo ESCALAB 250Xi). UV–Vis absorption spectra were carried out using UV–Vis Spectrophotometer SPECORD PLUS. Raman spectra were recorded using a Microscopic confocal Raman spectrometer (Horiba Jobin–Yvon LabRAM HR800) with an excitation length of 532 nm. The thermal conductivity was measured by TC3010 (Xi’an, China) using the transient hot wire method. All measurements were performed at room temperature.

3 Results and discussion

3.1 Power factor optimization of PEDOT:PSS films

Figure 2 shows the electrical conductivities, Seebeck coefficients and the power factors of PEDOT:PSS films

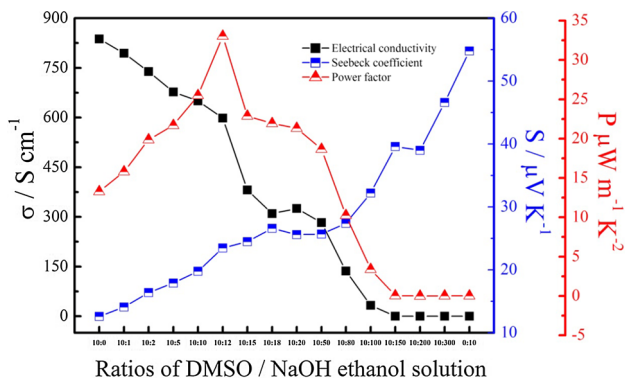


Fig. 2 Electrical conductivity, Seebeck coefficient and power factor of PEDOT:PSS films post-treated by DMSO/NaOH ethanol solution mixture with different volume ratios

during the optimizing process by DMSO/NaOH ethanol solution mixtures post treatment. The polymer film post-treated by single DMSO without NaOH component (10:0 volume ratio) displays an electrical conductivity of 837.2 S cm^{-1} , which is four orders of magnitude higher than that of pristine film (0.2 S cm^{-1}) and a seebeck coefficient of $12.6 \text{ } \mu\text{V K}^{-1}$, which is slightly lower than that of pristine film ($13.6 \text{ } \mu\text{V K}^{-1}$). This significantly enhanced electrical conductivity can be attributed to the phase separation between PEDOT and PSS chains because the utilized aprotic polar solvent DMSO with a high dielectric constant could induce a strong screening effect between charge carriers and counter ions, leading to the weakening of the Coulomb interaction between positively charged PEDOT and negatively charged PSS [26]. The introduction of NaOH in the form of NaOH ethanol solution could alternate acid PSS-H with neutralized PSS-Na thus effectively turning the Seebeck coefficient together with the electrical conductivity according to their anti-correlations. In fact, the mixture of DMSO/NaOH ethanol solution as a post-treatment reagent possesses the capacity of penetrating into the intermolecular sites between PEDOT and PSS and then results in a large dedoping effect. As observed in Fig. 2 (blue line), due to the dedoping effect, the Seebeck coefficient of PEDOT:PSS films gradually increases from 12.6 to $54.8 \text{ } \mu\text{V K}^{-1}$ as the volume ratio of NaOH ethanol solution in the mixture increases, whereas the electrical conductivity shows an decreasing tendency from 837.2 to 0.04 S cm^{-1} . Although the two parameters present an opposite tendency, we believe that such a facile dedoping technique and the extensive variation in the Seebeck coefficient, as well as the electrical conductivity, are crucial for understanding and outlining the desired optimized power factor. Based on the formula $P = \sigma S^2$, the power factors are calculated and

the corresponding curve (red line) is obtained. By varying the ratios between DMSO and NaOH ethanol solution, an optimal power factor of $33.04 \mu\text{W m}^{-1} \text{K}^{-2}$ appears at the ratio of 10:12 in volume due to the facile control of the dedoping level and the corresponding electrical conductivity and Seebeck coefficient are 598.2 S cm^{-1} and $23.5 \mu\text{V K}^{-1}$, respectively. Note that the obtained power factor is four orders of magnitude higher than that of the pristine PEDOT:PSS film as well as more than twice the value ($13.29 \mu\text{W m}^{-1} \text{K}^{-2}$) of DMSO post-treated film. Furthermore, this power factor is also much higher than the value ($19.6 \mu\text{W m}^{-1} \text{K}^{-2}$) from NaOH addition approach as reported by Tsai et al. [27].

3.2 Characterizations and mechanism for the TE enhancement of PEDOT:PSS films

To obtain information for the mechanism of electrical conductivity enhancement and to investigate the possible changes in the morphology and correlation between morphology and electrical conductivity, atomic force microscopy (AFM) characterization was conducted. Generally, it is believed that the bright and dark regions can be assigned to PEDOT and PSS phases, respectively [24, 34]. As presented in Fig. 3, phase image of the pristine PEDOT:PSS

film (Fig. 3a) is less contrastive and indicates that the PEDOT and PSS chains are uniformly blended, which leads to a weak phase separation between PEDOT and PSS hence the quite low electrical conductivity. Whereas a good phase separation between PEDOT and PSS chains occurs for the DMSO-treated film. The conducting PEDOT particles are further exposed and the conducting area becomes much larger than the pristine film, well confirming the remarkable electrical conductivity enhancement, as shown in Fig. 3b. The polymer film treated by DMSO/NaOH ethanol solution mixture (10:12) (Fig. 3c) also reveals phase separation relative to pristine film whereas with the PEDOT grains a bit less aggregated than DMSO-treated film. Hence the more PEDOT-rich regions effectively promote the electrical conductivity. In addition, the phase separation between PEDOT and PSS chains can be further evidenced by the roughening of the surface treated films relative to the pristine one, as observed in the height images (Fig. 3a–c) with the roughness (Rq) increasing from 1.36 nm to 2.52 nm and 2.02 nm.

In PEDOT:PSS, PSS is present in excess, insulator (non-ionized dopant) and the main reason for the low electrical conductivity of the commercial PEDOT:PSS. Selective removal of PSS is one of the mechanisms of electrical conductivity enhancement. Therefore, following the

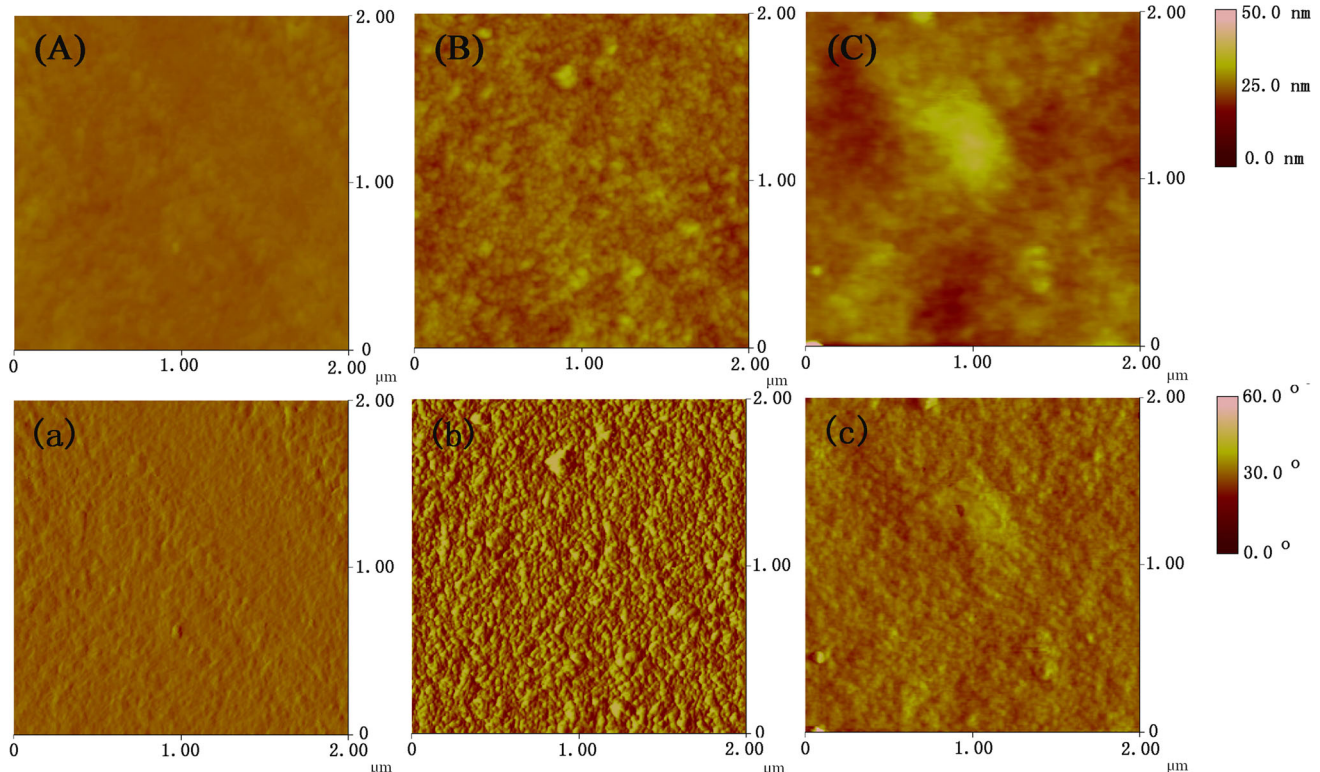
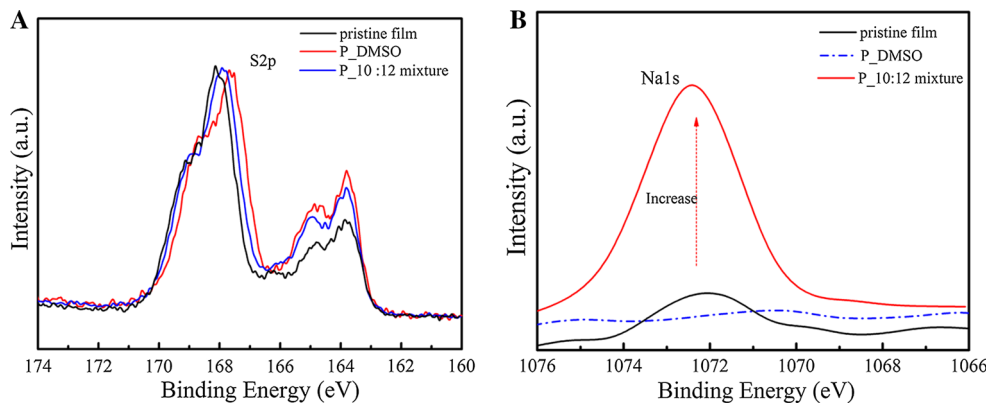


Fig. 3 AFM images of pristine PEDOT:PSS film (A, a) and those post-treated by DMSO/NaOH ethanol solution mixtures with different volume ratios: 10:0 mixture (B, b) and 10:12 mixture (C, c). *Upper row*: height images; *lower row*: phase images. Scanning area: $2 \mu\text{m} \times 2 \mu\text{m}$

Fig. 4 XPS spectra of pristine PEDOT:PSS film and those post-treated by DMSO/NaOH ethanol solution mixtures with different volume ratios. **a:** S(2*p*) spectra and **b:** Na(1*s*) spectra



morphology investigation, the effects of post-treatments on the surface compositions changes of PEDOT:PSS films were also analyzed using the X-ray photoelectron spectroscopy (XPS) technique. Figure 4a shows the S(2*p*) spectra of the pristine and post-treated PEDOT:PSS films. As observed, two characteristic sulfur (S) 2*p* peaks are detectable, the S(2*p*) peak at the higher binding energy of 167.8 and 169 eV corresponds to the sulphur signal of PSS and those at lower ones of 164.6 and 163.8 eV originates from the sulphur signal of PEDOT [35, 36]. Compared to the pristine film, the ratio of PEDOT to PSS increases for the films post-treated by DMSO and DMSO/NaOH ethanol solution mixture (10:12), implying the depletion of the PSS from the film surface. Additionally, the PEDOT to PSS ratio of DMSO-treated film is slightly more than the one treated by the mixture reagent, which is in agreement with the electrical conductivity enhancement. On the other hand, as shown in Fig. 4b, an increased Na1*s* signal from NaOH is detected in the spectrum of the film by the mixture (10:12) treatment, indicating the interaction between NaOH and PSSH, expressed by $PSS^{-}H^{+} + Na^{+}OH^{-} \rightarrow PSS^{-}Na^{+} + H_2O$, therefore the carrier density decreases due to the increased amount of PSS-Na which is poor at generating the carriers in comparison with PSSH and consequently introducing an improved Seebeck coefficient [27].

Raman spectra of pristine film and those post-treated by DMSO/NaOH solution mixtures with different volume ratios was performed to better understand the conformational changes and the effect of the reduction on the vibrational modes of PEDOT. Generally in Raman spectra, peak shifting to lower wavenumbers is due to an increase in the dedoping level and this effect is related to the degree of backbone deformation during reduction to polarons and neutral state and the associated transitions between quinoid- and benzoid-dominated forms [28, 37]. As shown in Fig. 5, the strongest band at 1435 cm^{-1} which is assigned to the symmetric $C_{\alpha}=C_{\beta}$ (-O) stretching gradually shifts to a lower wavenumber at 1427 cm^{-1} simultaneously with a

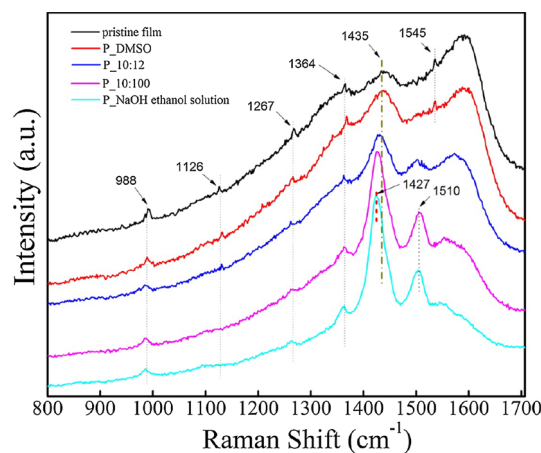


Fig. 5 Raman spectra of pristine PEDOT:PSS film and those post-treated by DMSO/NaOH ethanol solution mixtures with different volume ratios

peak narrowing as the NaOH content in the DMSO/NaOH solution mixtures increases, indicating the increase in the dedoping level of PEDOT chains from bipolaron to polaron or neutral state. In addition, during the dedoping process, the peak at 1545 cm^{-1} that can be found in the pristine and DMSO-treated film becomes weaker or disappeared while a new peak at 1510 cm^{-1} , which is assigned to the asymmetric $C_{\alpha}=C_{\beta}$ stretching, is grown for the dedoped films. Furthermore, the bands at 988, 1126, 1267 and 1364 cm^{-1} corresponds to the deformations of the oxyethylene ring, the PSS component, $C_{\alpha}=C_{\alpha}$ inter-ring stretching and $C_{\beta}=C_{\beta}$ stretching, respectively. Particularly, the observed intensity decrease at 988 and 1126 cm^{-1} suggest the decrease of the PSS component [5, 28, 38–40].

Figure 6 shows the UV–Vis absorption spectra (400 ~ 1100 nm) of the pristine PEDOT:PSS film and those through various post-treatments. As clearly seen, the optical spectra change systematically as a function of the NaOH content in the DMSO/NaOH ethanol solution mixture, indicating the change of the oxidation level of PEDOT chains. It is reported that the oxidation level is

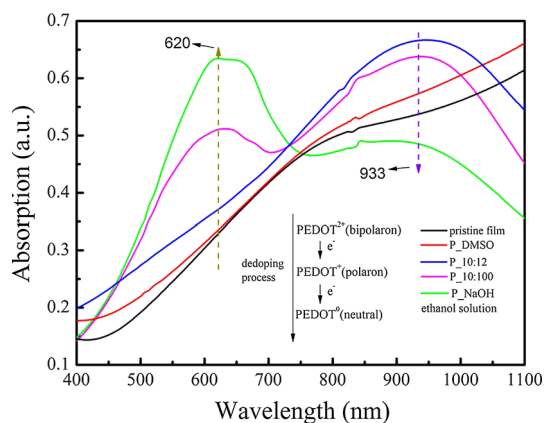


Fig. 6 UV–Vis spectra of pristine PEDOT:PSS film and those post-treated by DMSO/NaOH ethanol solution mixtures with different volume ratios

Table 1 Thermal conductivity of the samples at room temperature in this work

Sample	Thermal conductivity ($\text{W m}^{-1} \text{K}^{-1}$)	Refs.
Pristine PEDOT:PSS	0.170	[11]
DMSO-treated PEDOT:PSS	0.227	This work
DMSO/NaOH ethanol solution mixture(10:12)-treated PEDOT:PSS	0.173	This work
DMSO/NaOH ethanol solution mixture(10:100)-treated PEDOT:PSS	0.169	This work

crucial for the Seebeck coefficient of PEDOT [25]. During the dedoping process, PEDOT chains undergo three states (see the inset of Fig. 6), which show characteristic absorption at different wavelengths: in the near infrared region for PEDOT^{2+} (bipolaron), around 900 nm for PEDOT^+ (polaron) and around 600 nm for the neutral state, respectively [25, 41–45]. In Fig. 6, the spectra of the pristine and DMSO post-treated PEDOT:PSS films show a broad absorption band in the near infrared region (partly shown here), indicating the dominative role of the PEDOT^{2+} and no noticeable change is visible between them. As the volume ratio of NaOH ethanol solution to DMSO increases (NaOH content increases), the broad IR absorption background drastically diminishes in intensity while a broad polaronic transition peak increases at 933 nm, simultaneously a new transition emerges at 620 nm that originates from the absorption of neutral PEDOT segments of the polymer chains when the NaOH content is further increased. All these changes in the spectra suggest the dedoping of PEDOT chains from bipolaron states to polaron and then to neutral states, thus leading to the increase in the Seebeck coefficient.

3.3 Thermal conductivity and enhanced ZT value

It is recognized that the thermal conductivity of conducting polymers is dominated by the phonon transport and conducting polymers intrinsically possess low thermal conductivity typically ranging from 0.08 to $0.60 \text{ W m}^{-1} \text{K}^{-1}$, which is beneficial to the ZT enhancement [46–48]. In this work, the thermal conductivity at room temperature of the films through post-treatments was measured and listed in Table 1, which falls in the range of $0.169 \sim 0.227 \text{ W m}^{-1} \text{K}^{-1}$, approaching to the value of pristine PEDOT:PSS ($0.170 \text{ W m}^{-1} \text{K}^{-1}$) as previously reported [11]. Hence, as a general view, the dedoping method in our work achieves the optimization of power factor simultaneously maintaining quite low thermal conductivity, confirming the effectiveness of this technique as well as the recipe for post-treatment in improving the TE properties. In addition, according to the obtained optimal power factor ($33.04 \mu\text{W m}^{-1} \text{K}^{-2}$) before and the corresponding thermal conductivity ($0.173 \text{ W m}^{-1} \text{K}^{-1}$) measured here, the maximum ZT value is calculated to be 0.057 at RT, a relatively high value for organic TE materials.

4 Conclusion

In summary, we have reported an optimizing method that have improved the TE properties of PEDOT:PSS films by combining organic co-solvents with inorganic base as the post-treatment reagent, which achieves the facile combination of co-solvents effect and dedoping effect. By varying the ratios between DMSO and NaOH ethanol solution, an optimized ZT of 0.057 at RT is obtained at the volume ratio of 10:12, a relatively high value for organic TE materials, simultaneously with the corresponding electrical conductivity, Seebeck coefficient and thermal conductivity being 598.2 S cm^{-1} , $23.5 \mu\text{V K}^{-1}$ and $0.173 \text{ W m}^{-1} \text{K}^{-1}$, respectively. In addition, the electrical conductivity enhancement can be attributed to the removal of PSS insulators and the phase separation between PEDOT and PSS chains, the concomitant improvement in the Seebeck coefficient originates from the dedoping of PEDOT chains, which can be confirmed by various characterizations. All these results suggest that our dedoping technique is effective and promising for improving the TE properties of PEDOT:PSS films or other conducting polymers.

Acknowledgments This work was supported by the National Natural Science Foundation of China (51463008, 51303073, 51203070), the Science and Technology Landing Plan of Universities in Jiangxi province (KJLD12081), the Jiangxi Provincial Department of Science and Technology (20142BAB216032), and the Science and Technology Project of Jiangxi Science & Technology Normal university (2013XJYB001).

References

1. Y. Lan, A.J. Minnich, G. Chen, Z. Ren, *Adv. Funct. Mater.* **20**, 357–376 (2010)
2. D. Yoo, W. Son, S. Kim, J.J. Lee, S.H. Lee, H.H. Choi, J.H. Kim, *RSC Adv.* **4**, 58924–58929 (2014)
3. M. Zebarjadi, K. Esfarjani, M. Dresselhaus, Z. Ren, G. Chen, *Energy Env. Sci.* **5**, 5147–5162 (2012)
4. Y. Chen, Y. Zhao, Z. Liang, *Energy Env. Sci.* **8**, 401–422 (2015)
5. M. Culebras, C.M. Gomez, *J. Mater. Chem. A* **2**, 10109–10115 (2014)
6. F.F. Kong, C.C. Liu, J.K. Xu, F.X. Jiang, B.Y. Lu, R.R. Yue, G.D. Liu, J.M. Wang, *Chin. Phys. Lett.* **28**, 037201 (2011)
7. Q. Wang, Q. Yao, J. Chang, L. Chen, *J. Mater. Chem.* **22**, 17612–17618 (2012)
8. O. Bubnova, Z.U. Khan, A. Malti, S. Braun, M. Fahlman, M. Berggren, X. Crispin, *Nat. Mater.* **10**, 429–433 (2011)
9. O. Bubnova, Z.U. Khan, H. Wang, S. Braun, D.R. Evans, M. Fabretto, P. Hojati-Talemi, D. Dagnelund, J.-B. Arlin, Y.H. Geerts, *Nat. Mater.* **13**, 190–194 (2014)
10. Y. Du, S.Z. Shen, K. Cai, P.S. Casey, *Prog. Polym. Sci.* **37**, 820–841 (2012)
11. F.X. Jiang, J.K. Xu, B.Y. Lu, Y. Xie, R.J. Huang, L.F. Li, *Chin. Phys. Lett.* **25**, 2202 (2008)
12. G. Kim, L. Shao, K. Zhang, K. Pipe, *Nat. Mater.* **12**, 719–723 (2013)
13. R. Yue, J. Xu, *Synth. Met.* **162**, 912–917 (2012)
14. J. Luo, D. Billep, T. Waechtler, T. Otto, M. Toader, O. Gordan, E. Sheremet, J. Martin, M. Hietschold, D.R.T. Zahnd, T. Gessner, *J. Mater. Chem. A* **1**, 7576–7583 (2013)
15. G.J. Snyder, E.S. Toberer, *Nat. Mater.* **7**, 105–114 (2008)
16. Q. Jiang, C. Liu, H. Song, H. Shi, Y. Yao, J. Xu, G. Zhang, B. Lu, *J. Mater. Sci. Mater. Electron.* **24**, 4240–4246 (2013)
17. J.Y. Kim, J.H. Jung, D.E. Lee, J. Joo, *Synth. Met.* **126**, 311–316 (2002)
18. C. Liu, B. Lu, J. Yan, J. Xu, R. Yue, Z. Zhu, S. Zhou, X. Hu, Z. Zhang, P. Chen, *Synth. Met.* **160**, 2481–2485 (2010)
19. D.A. Mengistie, C.-H. Chen, K.M. Boopathi, F.W. Pranoto, L.J. Li, C.W. Chu, A.C.S. *Appl. Mater. Interfaces* **7**, 97–100 (2015)
20. N. Massonnet, A. Carella, O. Jaudouin, P. Rannou, G. Laval, C. Celle, J.P. Simonato, *J. Mater. Chem. C* **2**, 1278–1283 (2014)
21. T.C. Tsai, H.C. Chang, C.H. Chen, W.T. Whang, *Org. Electron.* **12**, 2159–2164 (2011)
22. C. Liu, J. Xu, B. Lu, R. Yue, F. Kong, *J. Electron. Mater.* **41**, 639–645 (2012)
23. H. Song, C. Liu, J. Xu, Q. Jiang, H. Shi, *RSC Adv.* **3**, 22065–22071 (2013)
24. T.C. Tsai, T.H. Chen, H.C. Chang, C.H. Chen, Y.C. Huang, W.T. Whang, *J. Polym. Sci. Part A Polym. Chem.* **52**, 3303–3306 (2014)
25. O. Bubnova, Z.U. Khan, A. Malti, S. Braun, M. Fahlman, M. Berggren, X. Crispin, *Nat. Mater.* **10**, 429–433 (2011)
26. H. Park, S.H. Lee, F.S. Kim, H.H. Choi, I.W. Cheong, J.H. Kim, *J. Mater. Chem. A* **2**, 6532–6539 (2014)
27. T.C. Tsai, H.C. Chang, C.H. Chen, Y.C. Huang, W.T. Whang, *Org. Electron.* **15**, 641–645 (2014)
28. S.H. Lee, H. Park, S. Kim, W. Son, I.W. Cheong, J.H. Kim, *J. Mater. Chem. A* **2**, 7288–7294 (2014)
29. S. Liu, H. Deng, Y. Zhao, S. Ren, Q. Fu, *RSC Adv.* **5**, 1910–1917 (2015)
30. S. Cheng, I. D’cruz, M. Wang, M. Leitch, C. Xu, *Energy Fuel* **24**, 4659–4667 (2010)
31. S. Javadian, H. Gharibi, H.T. Fallah, *J. Chem. Eng. Data* **55**, 1122–1130 (2010)
32. K. Kovács, G. Stampf, I. Klebovich, I. Antal, K. Ludányi, *Eur. J. Pharm. Sci.* **36**, 352–358 (2009)
33. N. Nanbu, S. Watanabe, M. Takehara, M. Ue, Y. Sasaki, *J. Electroanal. Chem.* **625**, 7–15 (2009)
34. C. Badre, L. Marquant, A.M. Alsayed, L.A. Hough, *Adv. Funct. Mater.* **22**, 2723–2727 (2012)
35. H. Kim, S. Nam, H. Lee, S. Woo, C.-S. Ha, M. Ree, Y. Kim, *J. Phys. Chem. C* **115**, 13502–13510 (2011)
36. G. Zotti, S. Zecchin, G. Schiavon, F. Louwet, L. Groenendaal, X. Crispin, W. Osikowicz, W. Salaneck, M. Fahlman, *Macromolecules* **36**, 3337–3344 (2003)
37. M. De Kok, M. Buechel, S. Vulto, P. Van de Weijer, E. Meulenlamp, S. De Winter, A. Mank, H. Vorstenbosch, C. Weijtens, V. Van Elsbergen, *Phys. Status Solidi A* **201**, 1342–1359 (2004)
38. S. Garreau, G. Louarn, J. Buisson, G. Froyer, S. Lefrant, *Macromolecules* **32**, 6807–6812 (1999)
39. M. Stavitska-Barba, A.M. Kelley, *J. Phys. Chem. C* **114**, 6822–6830 (2010)
40. J. Wang, K. Cai, S. Shen, *Org. Electron.* **17**, 151–158 (2015)
41. T.C. Chung, J. Kaufman, A. Heeger, F. Wudl, *Phys. Rev. B* **30**, 702 (1984)
42. T. Edwards, S. Sen, *J. Phys. Chem. B* **115**, 4307–4314 (2011)
43. S. Garreau, J. Duvail, G. Louarn, *Synth. Met.* **125**, 325–329 (2001)
44. J. Gustafsson, B. Liedberg, O. Inganäs, *Solid State Ion.* **69**, 145–152 (1994)
45. S.G. Im, K.K. Gleason, *Macromolecules* **40**, 6552–6556 (2007)
46. O. Bubnova, X. Crispin, *Energy Env. Sci.* **5**, 9345–9362 (2012)
47. M. Hu, D. Yu, J. Wei, *Polym. Test.* **26**, 333–337 (2007)
48. Q. Jiang, C. Liu, J. Xu, B. Lu, H. Song, H. Shi, Y. Yao, L. Zhang, *J. Polym. Sci. Part B Polym. Phys.* **52**, 737–742 (2014)